Environmental Engineering and Management Journal March 2021, Vol. 20, No. 3, 377-388
http://www.eemj.icpm.tuiasi.ro/; http://www.eemj.eu

"Gheorghe Asachi" Technical University of Iasi, Romania

APPLICATION OF THERMAL ANALYSIS TO IMPROVE THE PREPARATION CONDITIONS OF ZEOLITIC MATERIALS FROM FLYING ASH

Gabriela Buema[1], Gabriela Lisa[1], Olga Kotova[2], Gabriela Ciobanu[1], Liliana Ivaniciuc[1], Lidia Favier[3], Maria Harja[1*]

[1]"Gheorghe Asachi" Technical University of Iaşi, Faculty Chemical Engineering and Environmental Protection, 73 Prof. D. Mangeron Blvd., 700050, Iasi, Romania
[2]N.P. Yushkin Institute of Geology of the Komi Science Center of the Ural Branch of the Russian Academy of Sciences, Pervomayskaya st. 54, 167982, Syktyvkar, Russia
[3]University Rennes, Ecole Nationale Supérieure de Chimie de Rennes, CNRS, ISCR – UMR6226, F-35000 Rennes, France

Abstract

The aim of this study is to gain a better understanding of ash properties that makes it suitable for obtaining geopolymeric/zeolitic materials, as well as to demonstrate that thermal analysis can be used as an innovative procedure to compare different activation methods. Establishing a relationship between the physical and chemical characteristics of ash and materials obtained from fly ash is an important step towards producing large quantities of zeolitic materials with pre-established properties. In this paper, a direct relationship between TG analysis and the type of materials obtained from the local fly ash, by different methods, was proved for the first time. The experimental results demonstrated that the materials with a surface area over 40 m^2/g and pores volume over 0.12 cm^3/g exhibited the highest thermal loss. The samples exhibiting thermal loss over 10% contained zeolites phases, a fact confirmed by FT-IR and XRD, and more than 7% sodium in samples structure, as demonstrated by EDAX analysis. The results shown that thermal analysis allowed identification of the materials, as well as elucidation of the processes occurring during the thermal heating. Concordant to this study, the conditions for the optimum activation method consisted in: direct activation method, temperature equal to 363 ^oK, contact time 4 h, 1/3 solid/liquid ratio and use of 5M NaOH activation solution. It is known that TG/DTG analysis is an easy and the economic feasible method. TG analysis for establishing the zeolitization degree on the base of the number of stages (four stages), but more important, on the base of total mass losses (over 10%) is recommended.

Key words: activation, characterization, fly ash, thermal analysis, zeolite

Received: June, 2020; Revised final: December, 2020; Accepted: January, 2021; Published in final edited form: March, 2021

1. Introduction

In the context of the economic progress that relies on consumption, the replacement of raw materials with different wastes became a necessity (Brostow et al., 2020; Gholampour et al., 2020; Sutcu et al., 2019). The capitalization has an important environmental impact by saving raw materials and reducing pollution caused by storage. Taking into account the concept of sustainable development, the advanced capitalization of fly ash for obtaining zeolitic materials is recommended. The formation of these materials is highly dependent on the SiO_2/Al_2O_3 ratio of the base material.

The fly ash is a waste result from burning of coal in thermal power plants. Coal is one of the most used fuel for different purposes, being found worldwide (Gollakota et al., 2019) and will remain the most used fuel for producing energy. The annual production of fly ash worldwide is about 500 million

* Author to whom all correspondence should be addressed: e-mail: mharja@tuiasi.ro

tones (Kishor et al., 2020; Peng and Tonglin, 2018). Thermal power plants (TPP) generate large quantities of inorganic residues such as fly ash, bottom ash, slags and desulphurization waste which lead to environmental and health problems. These residues can contain different heavy metals and radionuclides that can be inhaled or ingested from drinking water (Lazarova et al., 2019). Consequently, finding ways of capitalizing the fly ash from thermal power plants is mandatory (Harja and Ciobanu, 2020).

The ash from TPP is the main industrial waste which, due to its chemical composition and hydraulic properties, constitutes a source for new raw materials that can be further used as building materials (Ghazali et al., 2019; Venkatakrishnaiah and Sakthivel, 2015; Yadav and Kumar Yadav, 2017), catalysts (Al-Zeer et al., 2019; Asl et al., 2018; Go and Yeom, 2019; Todorova et al., 2020; Wang et al., 2017); zeolites (Hałas et al., 2017; Harja et al., 2016; Izidoro et al., 2013; Kotova et al., 2017), stabilizers for land in certain areas (Ciocinta et al., 2013; Harja et al., 2016; Trivedi et al., 2013; Zgureva et al., 2020) as well as in different fields including synthesis of adsorbents for gas retention (Birley et al., 2019; Izquierdo and Querol, 2011); ceramics manufacture (Albertini et al., 2013; Goga et al., 2013; Ongwandee et al., 2020) and heavy metals removal (Asl et al., 2019; Harja et al., 2021; Meer and Nazir, 2018; Nguyen et al., 2018). However, literature reported both advantages and disadvanges/limitations regarding the use of ash for different applications (Bucur et al., 2014; Yao et al., 2015).

For converting fly ash into useful materials, different methods have been employed, such as: direct activation (Buema et al., 2014; Noli et al., 2015; Zhang et al., 2013), fusion (Javadian et al., 2015; Rios et al., 2009; Shoppert et al., 2017), microwave and ultrasound (Andac et al., 2005; Park et al., 2001).

The most important parameters in the transformation process are: activation time, activation solution concentration, temperature and ash/solution ratio (Curteanu et al., 2014). Different types of materials can result by parameter variation, but for producing eco-friendly materials the optimization of these conditions is crucial (Harja et al., 2016). The formation of these materials is also highly dependent on the SiO_2/Al_2O_3 ratio of the base material.

The aim of this study is to gain a better understanding of the process of ash converting in geopolymeric/zeolitic materials and proving that thermal analysis can be used as an innovative procedure to compare different activation methods.

The new materials were obtained using ash collected from TPP and subjected to different processes: direct activation, ultrasound and fusion methods. The resulted materials have been characterized by different analytical techniques. These methods are in generally costly and time consuming. The authors demonstrated that it is possible to establish the quality of obtained materials by an innovative procedure - thermal analysis. Establishing a relationship between the physical and chemical characteristics of both ash and resulting materials is an important step towards producing large quantities of zeolitic materials with pre-established properties.

2. Experimental

The fly ash used in this study, class F, with Si/Al ratio of 1.6, was collected from the Holboca thermal power plant, and it was characterized before usage (Harja et al., 2012; Harja et al., 2013). Within a previous study (Buema et al., 2020; Harja et al., 2008) it was determined that solid / liquid ratio between 1/3 and 1/5 are necessary for soaking the sample in order to ensure the environmental protection (the excess of water is lost to the washing water). Two concentrations of NaOH activation solution (Merck product) were chosen within this study: 2M and 5M. In order to obtain new ecofriendly materials the conditions presented in Table 1 were employed.

Described in detail, the activation and ultrasound methods involve 6 steps: mixing the components, activating fly ash by proper methods, cooling and crystallizing at room temperature for 18 h, filtering, washing at pH 8 with distilled water, drying at 80°C for 4 h. S1 material was synthesized for 168 hrs of contact time by direct activation method of 50 g of fly ash at 20^0C in 150 mL of 2 M of NaOH.

A quantity of fly ash was mixed with NaOH at a mass ratio of 1/5 using ultrasound method at 70^0C at different contact time. The materials obtained were noted as S2 and S3. For producing S4 and S5 materials, the classic method of direct activation was used. Fly ash was mixed with 5M of NaOH solution, 1/3 ratio, and heated at 90 °C for 4, and 15 h, respectively. For S6 material, 15 grams of fly ash and 45 g NaOH pellets were mechanically mixed. After grinding, the mixture was placed into muffle and synthesized at 150^0C for 150 h. Characterization of fly ash and resulted materials were performed in order to determine the chemical and mineralogical composition, morphology and surface area etc. that are necessary for various applications of fly ash.

Table 1. Optimum conditions for ash based ecofriendly materials

Samples	*Method*	*Ratio*	*Temperature, °C*	*NaOH, M*	*Curring time, h*
FA	***Raw ash***				
S1	Direct activation	1/3	20	2	168
S2	Ultrasound	1/5	70	5	1
S3	Ultrasound	1/5	70	5	2
S4	Direct activation	1/3	90	5	4
S5	Direct activation	1/3	90	5	15
S6	Fusion	1/3	150	Pellets	72

All materials were analyzed by: SEM/EDAX (Quanta 3D - AL99/D8229), XRD (X'Pert PRO MRD X-ray diffractometer), BET (Quanta-chrome Instruments), FT-IR (DIGILAB FTS2000), thermal analysis (METTLER TOLEDO TGA/ SDTA 851, 20 to 1000 °C, 10°C/60s).

3. Results and discussion

3.1. SEM analysis

SEM images for the obtained materials are shown in Fig. 1, which reveals that the result of treating the ash with NaOH is obvious. The new materials show significant changes on the surface following the alkaline activation, compared to the raw ash (Cretescu et al., 2018; Sarbak et al., 2004). Particles have different shapes, intersected and interconnected. The differences were influenced by the methods applied to each investigated material (Harja et al., 2009; Samiullah et al., 2018).

The properties of the new materials are influenced by the process temperature, since the increase of the temperature determines the acceleration of the chemical reactions that leads to modification of the crystalline lattice (Fig. 2). Significant changes were observed for S4 and S6 materials. These resulted by the direct activation at high temperatures, 90^0C and 150^0C respectively.

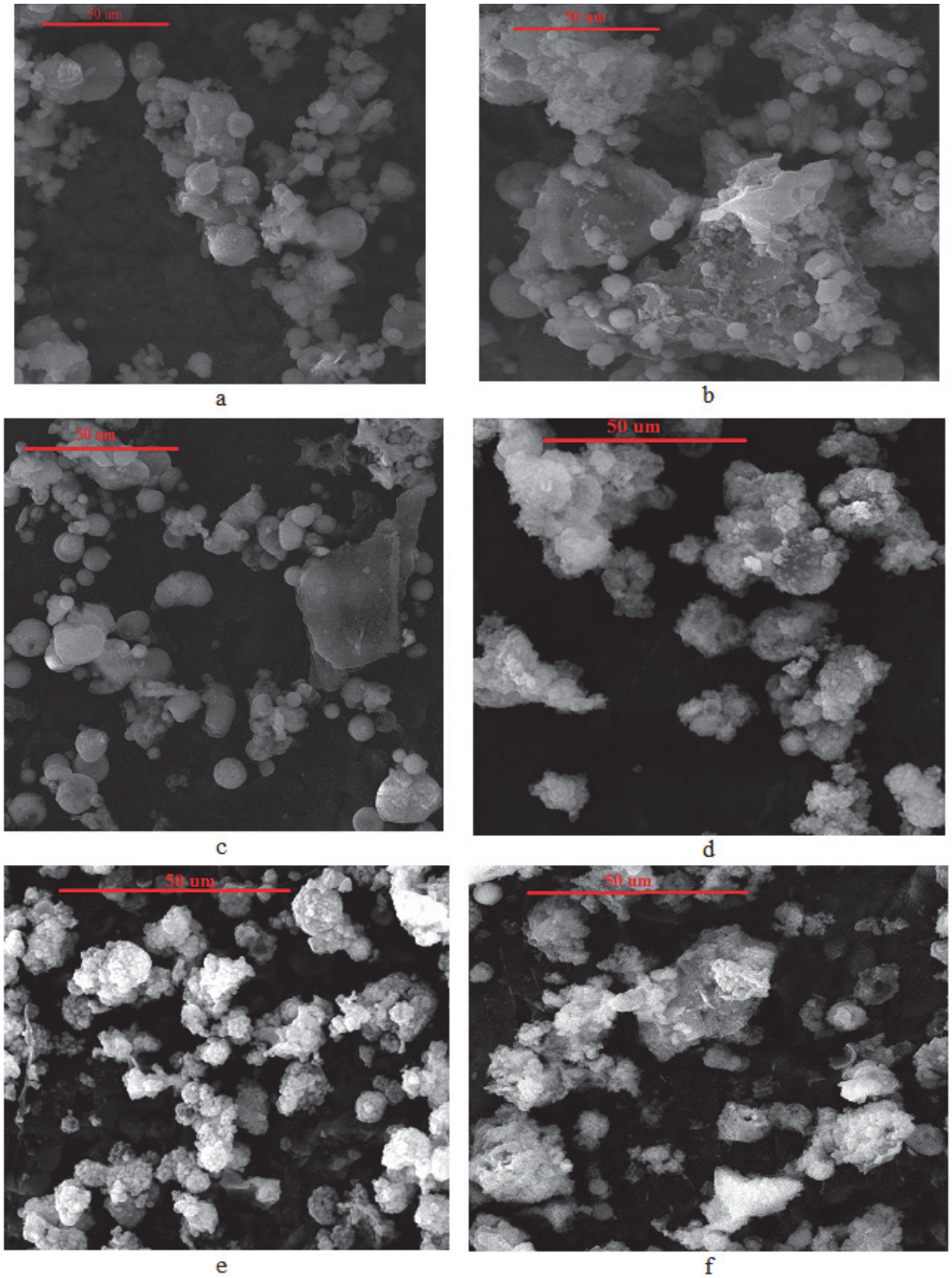

Fig. 1. SEM for the new materials: (a) represent S1, (b) represent S2, (c) represent S3, (d) represent S4, (e) represent S5 and (f) represent S6

Fig. 2 shows the fact that for S1 and S2 materials, the degree of transformation is reduced, while the direct activation under the selected conditions leads to an advanced transformation of the particles, in particular for S4 and S6 which exhibit a structure corresponding to zeolites.

The microstructure of sample S4, synthesized at 90^0C, is similar to that of sample S6, the difference resulting in the shape of the crystals, only. Heat treatment produces visible changes in the microstructure of the samples without significant differences in the elemental composition. The influence of the contact time is shown in Fig. 3. Thus, the SEM images revealed, the following aspects:

✓ the different morphologies of new materials depend on the process conditions;

✓ NaOH treatment using the ultrasound method resulted in a large number of uniformly distributed acicular particles. On the other hand, in the case of the materials modified by ultrasound, it is not recommended to increase the contact time, since by increasing the contact time the advanced destruction of the particles is achieved;

✓ new crystals of rhombic and cubic shapes, for S4;

✓ increase of the contact time led to crystal agglomerations (S5 and S6);

From the above results, one may conclude that the contact time between ash and NaOH is a very important step in obtaining materials with pre-established structures.

3.2. EDAX analysis

The average values of the chemical composition, EDAX, for the obtained materials are presented in Table 2. For comparison, the set of data for raw fly ash (FA) were included.

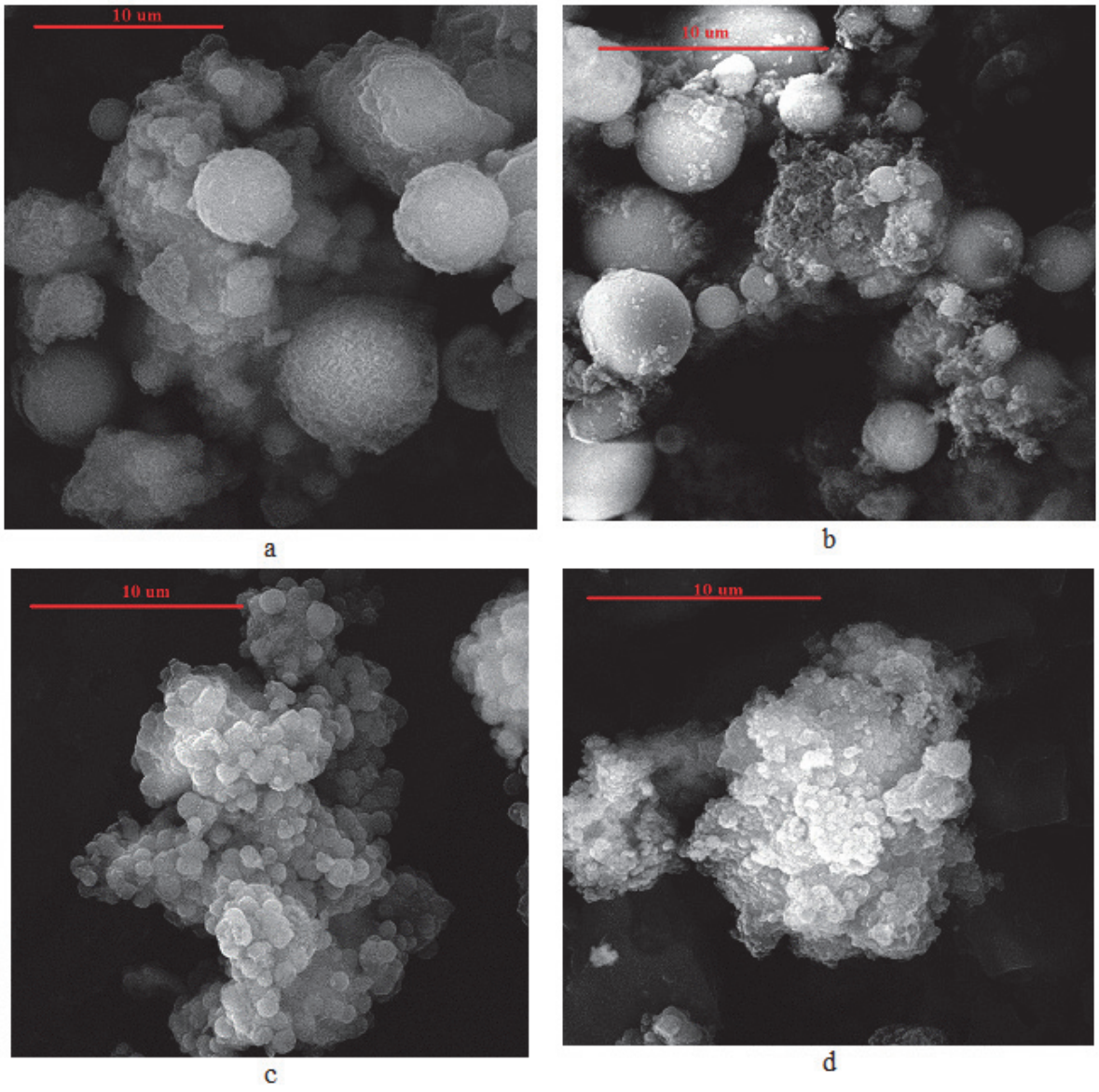

Fig. 2. The effect of temperature on the process: (a) represent S1, (b) represent S2, (c) represent S4 and (d) represent S6

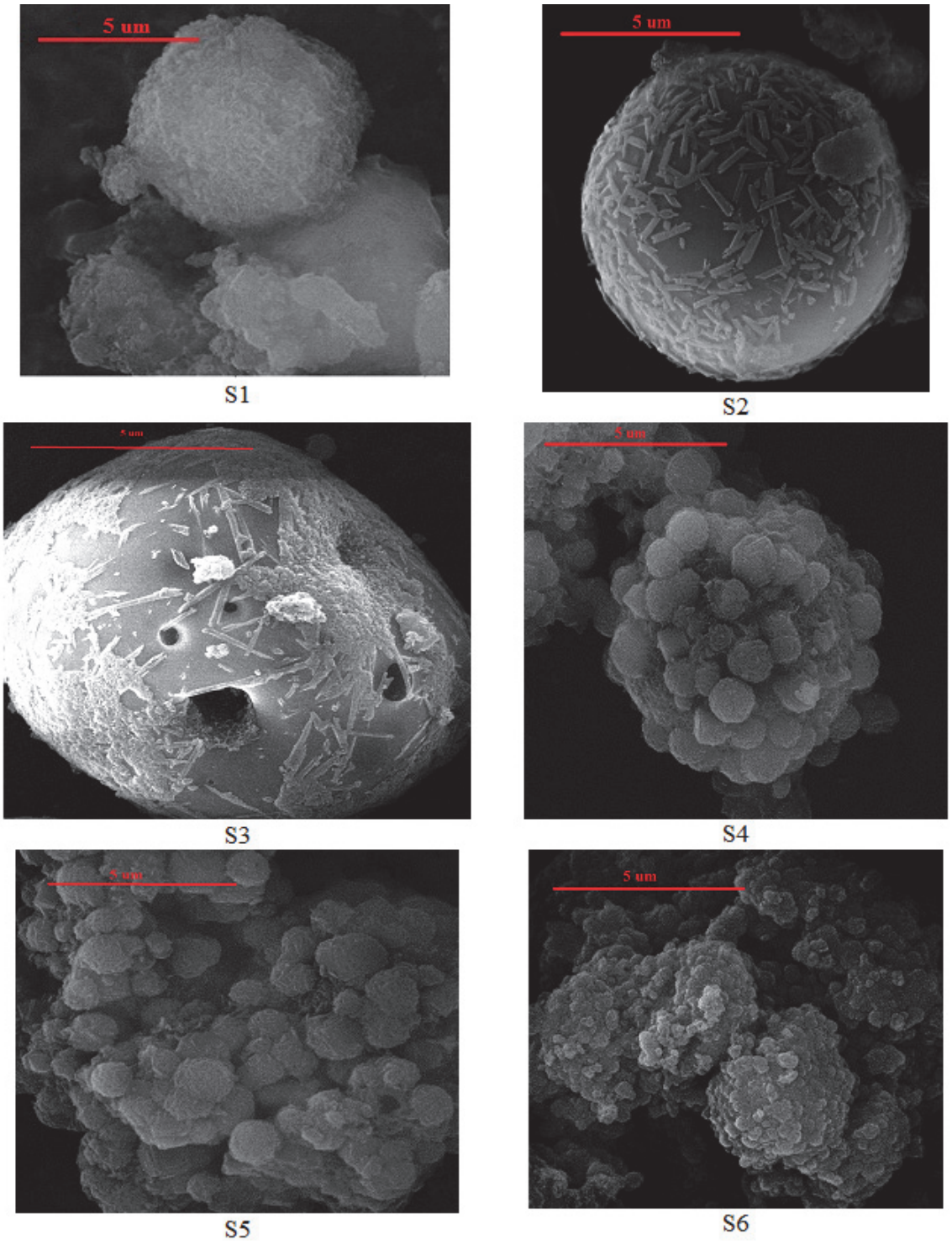

Fig. 3. The influence of contact time on the proces: (a) represent S1, (b) represent S2, (c) represent S3, (d) represent S4, (e) represent S5 and (f) represent S6

Table 2 shows that the sodium ion content increased due to the treatment of FA with 2M and 5 M, respectively, NaOH. The Si content of the new materials has decreased, as a result of the fact that this mineral dissolves during the alkaline attack. The SiO_2/Al_2O_3 ratio of the S1-S6 materials is smaller compared to that of the FA, which shows that the hydrothermal treatment contributes to the increase of the ion exchange capacity of these materials.

3.3. XRD and FTIR analysis

The identification of peaks was performed based on PCPDF Win (1999) and Collection of simulated XRD Powder Patterns for zeolites (Treacy and Higgins, 2001).

The obtained materials consist mainly of quartz, mulitte, hematite and magnetite as confirmed by the elementary chemical composition (Fig. 4). The

quartz and mulitte elements could not be completely dissolved during hydrothermal treatment. XRD analysis shows that the samples contain quartz (Q), mulitte (M), sodalite (S), feldspar (F), chabazite (Cha), clinotobermorite (CT), gismodine (Gis), Linde L (L), herchele (Her), faujasite (Fau), Na-Y, tobermorite (T) (Harja et al., 2015; Jin et al., 2018).

The new materials exhibit several diffraction peaks (Fig. 4). Also, one may observe that, in the case of materials obtained at low temperatures, the intensity of the quartz and iron peaks has been quite intense, fact which demonstrated a relatively low degree of zeolitization. This result is in accordance with the data presented by Querol et al., (2002) that have demonstrated that high temperatures are required in order to dissolve, completely or partially the Al -Si phases from the ash for obtaining new materials based on fly ash.

Significant peaks appear at 2 tetha= 6.25 0, 7.4 0, 7.54 0, 10.17 0, 10.45 0. These peaks correspond to S4, S5, and S6 materials. The new materials contain Analcime, but in small quantities. Aluminum is a structural element and its quantity influences the formation of new materials. Tobermorite element was formed in the case of the S4 material only. NaP1 zeolite formation is possible only in the case of the material obtained at a contact time of 15 hrs, and Na-Y in the case of materials S4, S5 and S6. Materials S5 and S6 also have peaks corresponding to the zeolites: Fau and Linde L. The FT-IR analysis (Fig. 5) confirms the results obtained by XRD. The FTIR vibration bands of the materials are presented in Table 3.

Table 2. The chemical composition for obtained materials (%)

Adsorbant	*O*	*Na*	*Mg*	*Al*	*Si*	*K*	*Ca*	*Ti*	*Fe*
FA	43.32	0.79	0.62	19.19	30.81	1.75	1.15	1.54	3.05
S1	33.85	3.44	0.93	18.33	28.89	0.66	1.44	0.91	4.07
S2	32.93	1.52	0.78	15.37	23.38	2.09	1.19	0.79	2.51
S3	34.13	1.78	1.06	15.55	24.64	1.71	1.39	1.03	3.87
S4	35.77	7.85	1.08	14.48	22.23	0.48	1.40	0.93	2.28
S5	38.37	10.87	1.28	15.31	24.10	0.71	1.69	0.82	2.97
S6	38.15	11.18	0.86	17.50	24.35	0.16	2.67	0.71	2.63

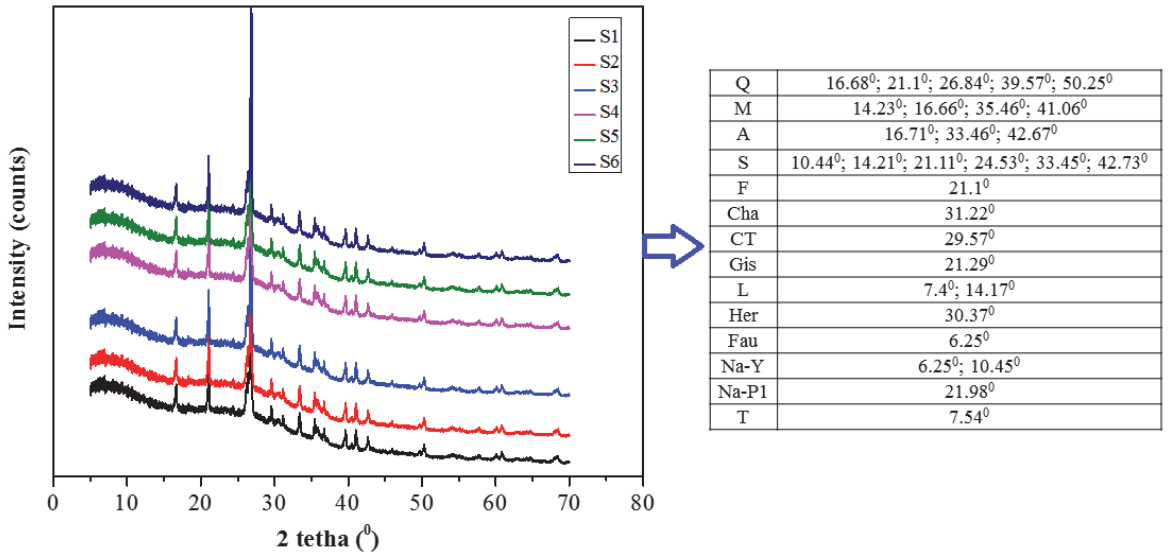

Q	16.68^0; 21.1^0; 26.84^0; 39.57^0; 50.25^0
M	14.23^0; 16.66^0; 35.46^0; 41.06^0
A	16.71^0; 33.46^0; 42.67^0
S	10.44^0; 14.21^0; 21.11^0; 24.53^0; 33.45^0; 42.73^0
F	21.1^0
Cha	31.22^0
CT	29.57^0
Gis	21.29^0
L	7.4^0; 14.17^0
Her	30.37^0
Fau	6.25^0
Na-Y	6.25^0; 10.45^0
Na-P1	21.98^0
T	7.54^0

Fig. 4. XRD analysis for fly ash and new materials S1 - S6 (Cards: T = 45-1480; CT = 45-1479; M = 79-1455; 83-1881; Q = 86-1629; A – 41-1478; 85-2066; F =84-0710; Cha = 85-1063; S = 85-2066; 85-2070; 86-1844) Q – quartz, Mu – mullite, S – sodalite, He – hematite, Cha – chabazite, HS – hydroxysodalite

Table 3. The vibration bands

Vibrational band range (cm^{-1})	*Assignment*
454-464	O - Si - O or Si - O - Si
556 - 559	Al - O - Si and Si - O - Si
695 – 699; 789 - 796	Si –O
734 - 796	Si - O - Si symmetrically
994-1094	Si - Al - O
1074 - 1086	Si - O - Si asymmetrical or T - O - Si asymmetric, where T = Si, Al
1635 – 1656; 3436 - 3448	OH, respectively H - O - H

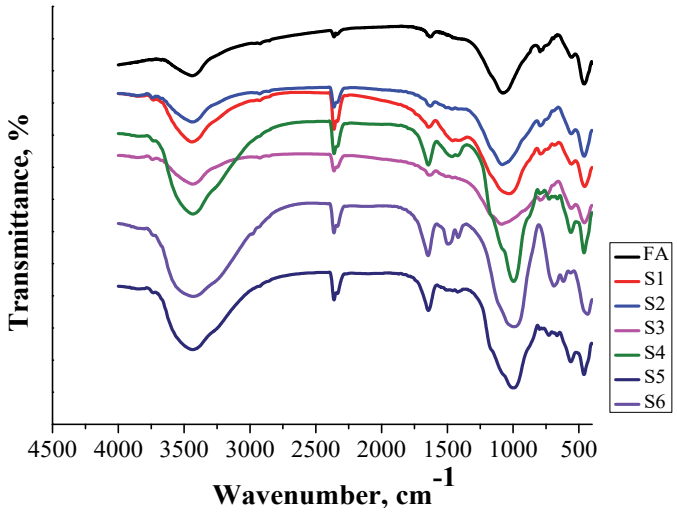

Fig. 5. FT-IR analysis for fly ash and new materials S1-S6

It should be noted that the peaks between 734 - 796 cm^{-1} can be attributed to the amorphous precursors of zeolites (Harja et al., 2009; Musyoka et al., 2012; You et al., 2019).

The results demonstrated that if the contact time and temperature increase, significant changes in the structure of materials are observed. FT-IR analysis of material S4 shows that it presents a peak at 1442 cm^{-1}, corresponding to the Na-Y zeolite, which is also confirmed by XRD analysis. S4 shows a peak corresponding to 2351 cm^{-1} wave number that is more pronounced compared to the FA. It is also observed in the peak shift from 1070 cm^{-1} to 994 cm^{-1} (for material S4) and 994 cm^{-1} (for S5). Material S5 has approximately the same values of the wave number as material S4, the differences consisting in the peak shift from 2351 cm^{-1} to 2367 cm^{-1} and the lack of the peak in the area 1442 cm^{-1}. More information can be found in several previous papers (Buema et al., 2014; Harja et al., 2012, 2013).

3.4. BET analysis

The values obtained for the specific surfaces of the new materials are presented in Table 3. According to the experimental results these materials exhibit a BET surface in the range 21-122 m^2/g. One may see that the specific surfaces and the pore volume increases for the new materials compared to FA material (Table 4). The S1 material has a large specific surface, which shows that the contact time is positive, but the small pore volume shows a crystalline agglomeration as a result of the fact that the transformation process was performed without agitation. The isotherms of synthesized materials are presented in Fig. 6.

The ultrasound method (S2 and S3) determines the increase of the specific surface up to 2, respectively 3 times. However, increasing the contact time from 1 to 2 hours does not show an improvement of the S_{BET}. On the contrary, for a contact time equal to 2 hrs the particles are destroyed, a fact that leads to negative effects on the growth of crystals. Increasing the temperature from 90^0C to 150^0C practically causes a twofold increase in the surface value. The high temperature (150 ^{0}C) and high contact time (72 hours) result in a material with a surface area 17 times higher and a pore volume 10 times higher compared to FA. The variation of volume pores is presented in Fig. 7. From Fig. 7 it can seen that the FA has a pore volume equal to 0.022 cm^3/g, while for the synthesized materials the value increases up to 0.247 cm^3/g.

3.5. TG and DTA analysis

The profile of the thermogravimetric curves is shown in the Fig. 8. According to the loss on ignition (LOI) and the DTG, in the case of FA the weight loss is a four-stage process: in the first stage (43.65 ^{0}C) the loss of humidity (0.74%) occurs; in the second stage (486 ^{0}C) the loss of crystallization water occurs (2.35%); in the third stage (675.75 ^{0}C) a loss of 1.31% occurs, corresponding to the oxidation of unburnt carbon from ash; in the fourth stage (820 ^{0}C), a loss of 2.12% occurs, corresponding to the presence of a small amount of $CaCO_3$ in ash.

For all new materials, thermal decomposition begins with water removal. The stages of thermal decomposition of ash, the activation energy – Ea - and the kinetic number - n corresponding to each stage are presented in Table 5. When direct activation and ultrasound methods are applied, the LOI values are higher for direct activation samples than for those resulted by ultrasonic method. The materials obtained by direct activation exhibit four stages of loss on ignition, and a LOI increase of 29.85%, depending on activation conditions, as Table 4 shows. By the use of DTG/DTA, the amount and nature of chemical species lost during the heating process are determined. The endothermic and exothermic peaks offer information regarding dehydration and amorphization/ recrystallization processes. The first exothermic peak represents the thermal stability.

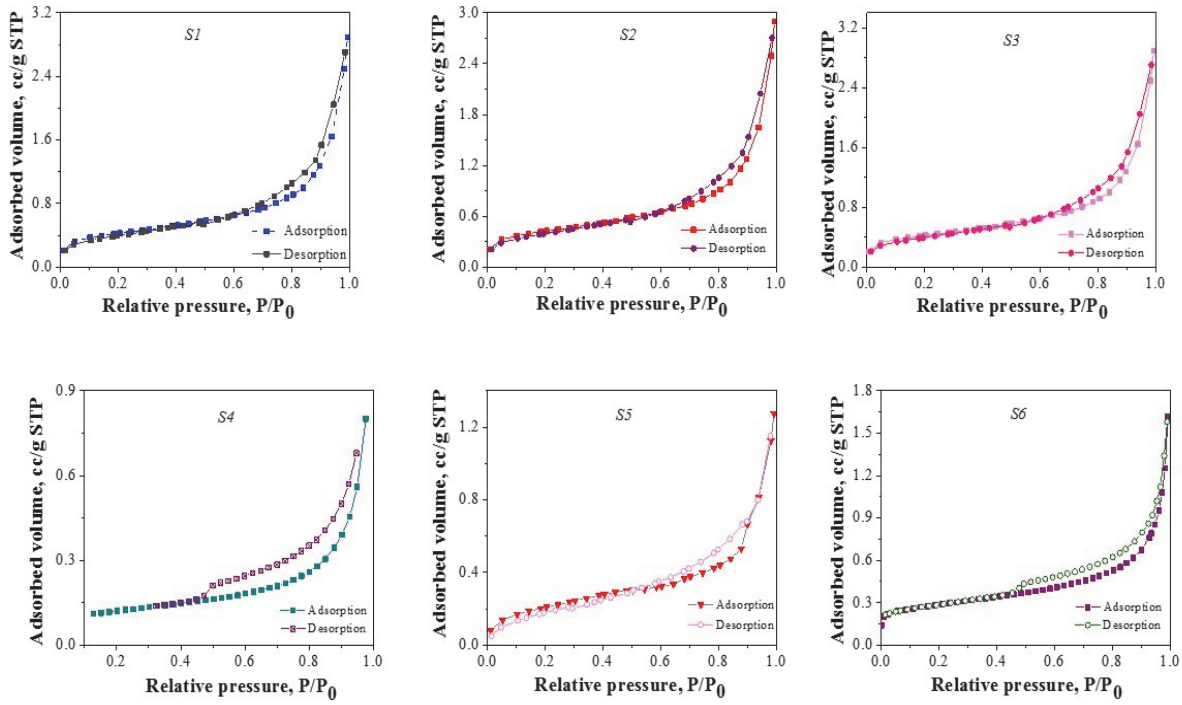

Fig. 6. The BET adsorption-desorption isotherm of S1 - S6

Table 4. BET specific surface values

Sample	***S_{BET}, m^2/g***
FA	7.53
S1	30.15
S2	20.52
S3	14.75
S4	40.18
S5	87.42
S6	121.63

The loss of the calcination occurs in four stages for FA, S1, S3 and S4 samples, in two stages for S5 and S6 samples and one stage for S2 sample. The S1 sample loss mass in the first and second stage, at 43.90 ^{0}C and 82.55 ^{0}C respectively, when losses of humidity of 1.81% and 2.22% respectively are achieved; in the third stage at 500.45 ^{0}C the loss of crystallization occurs (5.32%), whereas in the last stage at 778.72 ^{0}C a loss of 3.81% occurs, corresponding to the decarbonation of the structure.

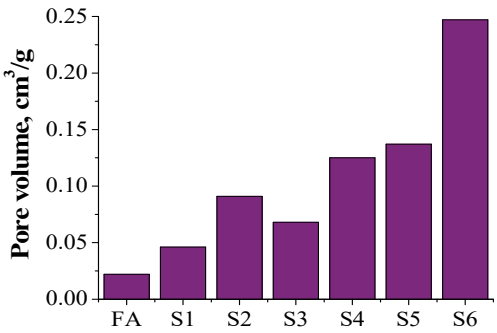

Fig. 7. The pore volume for analyzed materials

The S2 sample shows a total mass loss of about 2.3% at a temperature of 659.43^{0}C, when the lacks of crystal-hydrates are observed. The mass losses of the S3 material occur in 4 stages: in the first stage a mass loss of 1.72% occurs at the temperature of 45.38^{0}C, due to humidity; the second stage occurs from 478.4^{0}C with a mass loss of approximately 0.82%; the third stage occurs between 630.15^{0}C - 684.9^{0}C with a mass loss of 0.86%, and the last stage occurs at 769.97^{0}C with a loss of 3 % consisting in decarbonation of the structure.

For S4 the loss in calcination occurs in 4 stages: at a temperature of 46. 63^{0}C the mass loss is about 3.49%; at a temperature of 225^{0}C the mass loss is about 2%; at 536.21^{0}C the mass loss is 2.63% (the loss of crystallization water) and at temperature of 784.39^{0}C the mass loss is approximately 3.49%. The total mass loss was over 10%.

The S5 and S6 samples exhibit thermal decomposition in two stages, and total losses of 14.18%, and 29.85% respectively. The highest mass lost was achieved for sample obtained by the fusion method (S6), followed by samples obtained by direct activation (S4 and S5).

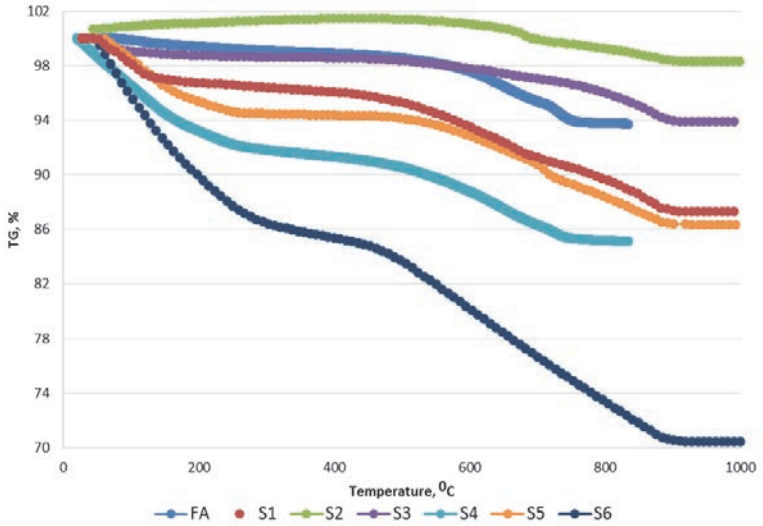

Fig. 8. Thermal analysis for FA and new materials

Table 5. The thermal degradation of the obtained materials

Sample	*Stage*	*Temperature, °C*		*A, kJ/ mol*	*Ea*	*n*	*Loss, %*	*Total loss, %*
		Ti, °C	*Tf, °C*					
FA	I	43.65	69.01	3.254	54.36	0.63	0.74	6.52
	II	486.42	665	$1.3 \cdot 10^{28}$	554.49	1.02	2.35	
	III	675.75	730.88	-	-	-	1.31	
	IV	820	900	-	-	-	2.12	
S1	I	43.90	65	-	-	-	1.81	9.06
	II	82.55	132.27	$0.4294 \cdot 10^{2}$	23.43	0.62	2.12	
	III	500.45	678.11	$2.54 \cdot 10^{14}$	297.69	1.72	2.32	
	IV	778.72	900	-	-	-	3.81	
S2	I	659.43	695.45	$1.54 \cdot 10^{28}$	551.38	0.96	2.2697	2.27
S3	I	45.38	98.14	$7.4582 \cdot 10^{8}$	68.11	2.04	1.7253	6.46
	II	478.40	520	-	-	-	0.8176	
	III	630	684.90	$1.36 \cdot 10^{10}$	219.50	0.86	0.8584	
	IV	769.97	900	-	-	-	3.0601	
S4	I	46.63	144.45	-	-		3.4884	10.71
	II	225	239.35	$0.9654 \cdot 10^{2}$	32.33	2.30	1.9871	
	III	536.21	690.98	-	-	-	2.6329	
	IV	784.39	900	-	-	-	2.6057	
S5	I	50.77	243.89	$0.3087 \cdot 10^{2}$	29.36	2.02	6.14	14.18
	II	536.60	900	$1.43 \cdot 10^{12}$	271.72	1.23	8.04	
S6	I	50.40	278.67	$2.67 \cdot 10^{2}$	31.03	0.74	14.5924	29.85
	II	477.86	900	-	-	-	15.2574	

Thermal analysis allows the identification of the materials as well as the elucidation of the processes occurring during the thermal heating, for establishing the optimum activation method. The obtained results are in agreement with literature (Grela et al., 2016).

The results of adsorption capacities indicated that the new obtained materials are very efficient in heavy metals removal (Buema et al., 2014; Harja et al., 2012; Harja et al., 2013; Noli et al., 2015). The zeolites obtained by direct activation are more efficient (a fact demonstrated by adsorption capacities), exhibit a higher level of hydration and four stages of dehydration. On the base of experimental results, by corroborating all information one concluded that high surface area and pores volume correspond to high thermal loss. The samples S4-S6 contain zeolites phases, confirmed by FT-IR and XRD. These materials have a very good adsoption properties, as demonstrated in a previous paper (Harja and Ciobanu, 2020), but for the first time a direct relantionship between TG analysis and material properties was found.

4. Conclusions

Since the capitalization of fly ash is very important for reduction of environmental pollution, the possibility to capitalize the fly ash from a thermal power plant has been examined. Within the current paper, the use of thermal analysis in order to determine the zeolitization degree for materials obtained from thermal power plant ashes, as well as to establish the

optimal transformation conditions was presented as a novelty.

Thermal analysis allows both identification of the materials and elucidation of the processes occurring during the thermal heating, in order to establish the optimum activation method.

Fly ash from coal combustion is not yet widely used in industry. Zeolites and zeolites precursor from the fly ash by alkaline conversion have been obtained. The contact time between ash and NaOH is a very important step in obtaining materials with structure corresponding to zeolites. According to the experimental results, the new materials exhibit a BET surface area between 21-122 m^2/g. FT-IR and XRD analysis demonstrated that the new materials contain: quartz, analcime, sodalite, chabazite, faujasite, Na-Y, tobermorite-mixtures of geopolymers/zeolites phases.

It is known that TG/DTG analysis is an easy and economic feasible method. Thermal analysis demonstrated that fly ash and materials obtained by ultrasound methods exhibit total loss up to 6%, compared to initial fly ash. The materials resulted by direct activation and fusion method, respectively, present four stages in thermal process, while total loss was ranged between 9 and 29%, as function of process conditions. The experimental results demonstrated that a total mass loss over 10% leads to materials with high zeolitization degree.

The TG analysis is recommended for establishing the zeolitization degree, on the base of the number of stages, but more important, on the base of total mass loss. This easy and economic feasible method allows the possibility to rapidly establish the period of alkaline attack process, on the base of the total mass loss only. The total mass loss over 10% denotes that the obtained materials exhibit a zeolitic structure. A direct relationship between TG analysis and material properties was proved. The general recommended method for obtaining new materials is direct activation, as they have advantages both economically and practically.

References

Albertini A.V.P., Silva J.L., Freire V.N., Santos R.P., Martins J.L., Cavada B.S., Cadena P.G., Rolim Neto P.J., Pimentel M.C.B., Martínez C.R., Porto A.L.F., Lima Filho J.L., (2013), Immobilized invertase studies on glass–ceramic support from coal fly ashes, *Chemical Engineering Journal*, **214**, 91-96.

Al-Zeer M.I.M., MacKenzie K.J.D., (2019), Fly ash-based geopolymers as sustainable bifunctional heterogeneous catalysts and their reactivity in Friedel-Crafts acylation reactions, *Catalysts*, **9**, 372-385.

Andac O., Tather M., Sirkecioglu A., Ece I., Erdem-Senatalar A., (2005), Effects of ultrasound on zeolite: A synthesis, *Microporous Mesoporous Materials*, **79**, 225-233.

Asl S.M.H., Ghadi A., Sharifzadeh Baei M., Hamedreza Javadian H., Maghsudi M., Kazemian H., (2018), Porous catalysts fabricated from coal fly ash as cost-effective alternatives for industrial applications: A review, *Fuel*, **217**, 320-342.

Asl S.M.H., Javadian H., Khavarpour M., Belviso C., Taghavi M., Maghsudi, M., (2019), Porous adsorbents derived from coal fly ash as cost-effective and environmentally-friendly sources of aluminosilicate for sequestration of aqueous and gaseous pollutants: A review, *Journal of Cleaner Production*, **208**, 1131-1147.

Birley R.I., Jones J.M., Darvell L.I., Williams A., Waldron D.J., Levendis Y.A., Rokni E., Panahi A., (2019), Fuel flexible power stations: Utilisation of ash co-products as additives for NO_x emissions control, *Fuel*, **251**, 800-807.

Brostow W., Chetuya N., Gencel O., Hong H.J., Menard N., Sayana, S., (2020), Durability of portland concrete containing polymeric fillers and fly ash, *Materials Science*, **26**, 103-108.

Bucur R.D., Cimpeanu C., Barbuta M., Ciobanu G., Paraschiv G., Harja M., (2014), A comprehensive characterization of ash from Romania thermal power plant, *Journal of Food, Agriculture and Environment*, **12**, 943-949.

Buema G., Misaelides P., Noli F., Sutiman D.M., Cretescu I., Harja M., (2014), Uranium removal from aqueous solutions by raw- and modified power plant ash, *Journal of Radioanalytical and Nuclear Chemistry*, **299**, 381-386.

Buema G., Lupu N., Chiriac H., Roman T., Porcescu M., Ciobanu G., Burghila D.V., Harja M., (2020), Eco-friendly materials obtained by fly ash sulphuric activation for cadmium ions removal, *Materials*, **13**, 3584, http://doi.org/10.3390/ma13163584.

Ciocinta R.C., Harja M., Bucur D., Buema G., (2013), Optimization of the conditions for conversion of coal ash into zeolite material, *Journal of Food, Agriculture & Environment*, **11**, 1108-1112.

Cretescu I., Harja M., Teodosiu C., Isopescu D.N., Chok M.F., Sluser B.M., Salleh M.A.M., (2018), Synthesis and characterisation of a binder cement replacement based on alkali activation of fly ash waste, *Process Safety and Environmental Protection*, **119**, 23-35.

Curteanu S., Buema G., Piuleac C.G., Sutiman D.M., Harja M., (2014), Neuro-evolutionary optimization methodology applied to the synthesis process of ash based adsorbents, *Journal of Industrial and Engineering Chemistry*, **20**, 597-604.

Gollakota A.R., Volli V., Shu C.M., (2019), Progressive utilisation prospects of coal fly ash: A review, *Science of Total Environment*, **672**, 951-989.

Ghazali N., Muthusamy K., Ahmad S.W., (2019), *Utilization of Fly Ash in Construction,* IOP Conf. Series: Materials Science and Engineering, **601**, 012023, http://doi.org/10.1088/1757-899X/601/1/012023.

Gholampour A., Ozbakkaloglu T., Gencel O., Ngo T.D., (2020), Concretes containing waste-based materials under active confinement, *Construction and Building Materials*, **270**, 121465, http://doi.org/10.1016/j.conbuildmat.2020.121465.

Go Y.W., Yeom S.H., (2019), Fabrication of a solid catalyst using coal fly ash and its utilization for producing biodiesel, *Environmental Engineering Research*, **24**, 324-333.

Goga F., Dudric R., Cormos C., Imre F., Bizo L., Misca R., (2013), Fly ash from thermal power plant, raw material for glass-ceramic, *Environmental Engineering and Management Journal*, **12**, 337-342.

Grela A., Łach M., Mikuła J., Hebda M., (2016), Thermal analysis of the products of alkali activation of fly ash

from CFB boilers, *Journal of Thermal Analysis and Calorimetry*, **124**, 1609-1621.

Hałas P., Kołodynska D., Płaza A., Geca M., Hubicki Z., (2017), Modified fly ash and zeolites as an effective adsorbent for metal ions from aqueous solution, *Adsorption Science & Technology*, **35**, 519-533.

Harja M., Barbuta M., Rusu L., Apostolescu N., (2008), Utilization of coal fly ash from power plants I. Ash characterization, *Environmental Engineering and Management Journal*, **7**, 289-293.

Harja M., Barbuta M., Gavrilescu M., (2009), Study of morphology for geopolymer materials obtained from fly ash, *Environmental Engineering and Management Journal*, **8**,1021-1027.

Harja M., Buema G., Sutiman D.M., Munteanu C., Bucur D., (2012), Low cost adsorbents obtained from ash for copper removal, *Korean Journal of Chemical Engi*neering, **29**, 1735-1744.

Harja M., Buema G., Sutiman D.M., Cretescu I., (2013), Removal of heavy metal ions from aqueous solutions using low-cost sorbents obtained from ash, *Chemical Papers*, **67**, 497-508.

Harja M., Buema G., Bulgariu L., Bulgariu D., Sutiman D.M., Ciobanu G., (2015), Removal of cadmium (II) from aqueous solution by adsorption onto modified algae and ash, *Korean Journal of Chemical Engineering*, **32**, 1804-1811.

Harja M., Cimpeanu S.M., Dirja M., Bucur D., (2016), *Synthesis of Zeolite from Fly Ash and their Use as Soil Amendment*, In: *Zeolites: Useful Minerals*, 43-66, doi:10.5772/64126.

Harja M., Buema G., Lupu N., Chiriac H., Herea D.D., Ciobanu G., (2021), Fly ash coated with magnetic materials: improved adsorbent for Cu (II) removal from wastewater, *Materials*, **14**, 63.

Harja M., Ciobanu G., (2020), *Eco-Friendly Nano-Adsorbents for Pollutant Removal from Wastewaters*, In: *Handbook of Nanomaterials and Nanocomposites for Energy and Environmental Applications,* Kharissova O., Martínez L., Kharisov B. (Eds), Springer, Cham, 1-22, https://doi.org/10.1007/978-3-030-11155-7_68-1

Izidoro J., Fungaro D., Abbott J., Wang S., (2013), Synthesis of zeolites X and A from fly ashes for cadmium and zinc removal from aqueous solutions in single and binary ion systems, *Fuel*, **103**, 827–834.

Izquierdo M., Querol X., (2011), Leaching behaviour of elements from coal combustion fly ash: an overview, *International Journal of Coal Geology*, **94**, 54-66.

Javadian H., Ghorbani F., Tayebi H., Asl S.M., (2015), Study of the adsorption of Cd (II) from aqueous solution using zeolite-based geopolymer, synthesized from coal fly ash: kinetic, isotherm and thermodynamic studies, *Arabian Journal of Chemistry*, **8**, 837-849.

Jin H., Liu Y., Wang C., Lei X., Guo M., Cheng F., Zhang, M., (2018), Two-step modification towards enhancing the adsorption capacity of fly ash for both inorganic Cu (II) and organic methylene blue from aqueous solution, *Environmental Science and Pollution Research*, **25**, 36449-36461.

Kishor M.S.V.R., Behera A., Rajak D.K., Pradeep L.M., Pruncu I.C, (2020), Manufacturing and mechanical characterization of cly-csh-reinforced Materials for furnace lining applications, *Journal of Materials Engineering and Performance*, **29**, 6307-6321.

Kotova O.B., Harja M., Cretescu I., Noli F., Pelovski Y., Shushkov D.A., (2017), Zeolites in technologies of pollution prevention and remediation of aquatic systems, *Vestnik IG Komi SC UB RAS*, **5**, 49-53.

Lazarova K., Boycheva S., Vasileva M., Zgureva D., Georgieva B., Babeva T., (2019), Zeolites from fly ash embedded in a thin niobium oxide matrix for optical and sensing applications, *Journal of Physics: Conference Series*, **1186**, 012024, http://doi.org/10.1088/1742-6596/1186/1/012024.

Meer I., Nazir R., (2018), Removal techniques for heavy metals from fly ash, *Journal of Material Cycles and Waste Management*, **20**, 703-722.

Musyoka N., Petrik L., Hums E., Baser H., Schwieger W., (2012), In situ ultrasonic monitoring of zeolite: A crystallization from coal fly ash, *Catalysis Today*, **190**, 38-46.

Nguyen T.C., Loganathan P., Nguyen T.V., Kandasamy J., Naidu R., Vigneswaran S., (2018), Adsorptive removal of five heavy metals from water using blast furnace slag and fly ash, *Environmental Science and Pollution Research*, **25**, 20430-20438.

Noli F., Buema G., Misaelides P., Harja M., (2015), New materials synthesized from ash under moderate conditions for removal of toxic and radioactive metals, *Journal of Radioanalytical and Nuclear Chemistry*, **303**, 2303-2311.

Ongwandee M., Namepol K., Yongprapat K., Homwuttiwong S., Pattiya A., Morris J., Chavalparit, O., (2020), Coal bottom ash use in traditional ceramic production: evaluation of engineering properties and indoor air pollution removal ability, *Journal of Material Cycles and Waste Management*, **22**, 2118-2129.

Park J., Kim B.C., Park A.S., Park H.C., (2001), Conventional versus ultrasonic synthesis of zeolite 4A from kaolinite, *Journal of Materials Science Letters*, **20**, 531-533.

Peng X., Tonglin Z., (2018), Comprehensive utilization of high alumina coal fly ash under the recyclable economy model, *Industrial Chemistry*, **4**, http://doi.org/10.4172/2469-9764.1000128.

Querol X., Moreno N., Umaña J.C., Alastuey A., Hernandez E., Lopez-Soler A., Plana F., (2002), Synthesis of zeolites from coal fly ash: An overview, *International Journal of Coal Geology*, **50**, 413-423.

Rios C., Williams C., Roberts C., (2009), A comparative study of two methods for the synthesis of fly ash-based sodium and potassium type zeolites, *Fuel*, **88**, 1403–1416.

Samiullah M., Aslam Z., Rana A.G., Abbas A., Ahmad W., (2018), Alkali-activated boiler fly ash for Ni (II) removal: Characterization and parametric study, *Water, Air, & Soil Pollution*, **229**, 113.

Sarbak Z., Stanczyk A., Kramer-Wachowiak M., (2004), Characterization of surface properties of various fly ashes, *Powder Technology*, **145**, 82-87.

Shopper A., Loginova I., Chaikin L., Rogozhnikov D., (2017), Alkali fusion-leaching method for comprehensive processing of fly ash, *KnE Materials Science*, **2**, 89-96.

Sutcu M., Erdogmus E., Gencel O., Gholampour A., Atan E., Ozbakkaloglu, T., (2019), Recycling of bottom ash and fly ash wastes in eco-friendly clay brick production, *Journal of Cleaner Production*, **233**, 753-764.

Todorova S., Barbov B., Todorova T., Kolev H., Ivanova I., Shopska M., Yuri Kalvachev Y., (2020), CO oxidation over Pt-modified fly ash zeolite X, *Reaction Kinetics, Mechanisms and Catalysis*, **129**, 773-786.

Trivedi J., Nair S., Iyyunni C., (2013), Optimum utilization of fly ash for stabilization of sub-grade soil using genetic algorithm, *Procedia Engineering*, **51**, 250-258.

Venkatakrishnaiah R., Sakthivel G., (2015), Bulk utilization of fly ash in self compacting concrete, *KSCE Journal of Civil Engineering*, **19**, 2116-2120.

Wang N., Chen J., Zhao Q., Xu H., (2017), Study on preparation conditions of coal fly ash catalyst and catalytic mechanism in a heterogeneous Fenton-like process, *RSC Advances*, **7**, 52524-52532.

Yadav A., Kumar Yadav N., (2017), Study of fly ash cement concrete pavement, *International Journal of Civil Engineering*, **4**, 1-6.

Yao Z.T., Ji X.S., Sarker P.K, Tang J.H., Ge L.Q., Xia M.S., Xi Y.Q., (2015), A comprehensive review on the applications of coal fly ash, *Earth-Science Reviews*, **141**, 105-121.

You S., Ho S.W., Li T., Maneerung T., Wang C.H., (2019), Techno-economic analysis of geopolymer production from the coal fly ash with high iron oxide and calcium oxide contents, *Journal of Hazardous Materials*, **361**, 237-244.

Zgureva D., Boycheva S., Behunová D., Václavíková M., (2020), Smart-and zero-energy utilization of coal ash from thermal power plants in the context of circular economy and related to soil recovery, *Journal of Environmental Engineering*, **146**, 04020081, http://doi.org/10.1061/(ASCE)EE.1943-7870.0001752.

Zhang X., Tang D., Jiang G., (2013), Synthesis of zeolite NaA at room temperature: The effect of synthesis parameters on crystal size and its size distribution, *Advanced Powder Technology*, **24**, 689-696.